Journal of Hazardous Materials 209–210 (2012) 458–466

Contents lists available at SciVerse ScienceDirect

Journal of Hazardous Materials

journal homepage: www.elsevier.com/locate/jhazmat

Sequestration of carbon dioxide by indirect mineralization using Victorian brown coal fly ash

Yong Sun, Vinay Parikh, Lian Zhang*

Department of Chemical Engineering, Monash University, Wellington Road, Clayton, GPO Box 36, Victoria 3800, Australia

ARTICLE INFO

Article history:
Received 11 October 2011
Received in revised form
22 December 2011
Accepted 16 January 2012
Available online 23 January 2012

Keywords:
Vitorian brown coal fly ash
Mineralization
CO_2 sequestration

ABSTRACT

The use of an industry waste, brown coal fly ash collected from the Latrobe Valley, Victoria, Australia, has been tested for the post-combustion CO_2 capture through indirect minersalization in acetic acid leachate. Upon the initial leaching, the majority of calcium and magnesium in fly ash were dissolved into solution, the carbonation potential of which was investigated subsequently through the use of a continuously stirred high-pressure autoclave reactor and the characterization of carbonation precipitates by various facilities. A large CO_2 capture capacity of fly ash under mild conditions has been confirmed. The CO_2 was fixed in both carbonate precipitates and water-soluble bicarbonate, and the conversion between these two species was achievable at approximately 60 °C and a CO_2 partial pressure above 3 bar. The kinetic analysis confirmed a fast reaction rate for the carbonation of the brown coal ash-derived leachate at a global activation energy of 12.7 kJ/mol. It is much lower than that for natural minerals and is also very close to the potassium carbonate/piperazine system. The CO_2 capture capacity of this system has also proven to reach maximum 264 kg CO_2/tonne fly ash which is comparable to the natural minerals tested in the literature. As the fly ash is a valueless waste and requires no comminution prior to use, the technology developed here is highly efficient and energy-saving, the resulting carbonate products of which are invaluable for the use as additive to cement and in the paper and pulp industry.

1. Introduction

Post-combustion CO_2 capture (PCC) is one of the promising options for a quick mitigation of the greenhouse gas emitted from power plants for the combustion of fossil fuels such as coal [1]. The conventional concept for PCC consists of an initial on-site separation and compression of CO_2 and subsequent transportation of CO_2 to an appropriate storage site such as depleted oil fields or aquifers. Such a way requires a costly and energy-intensive surveillance for the prevention of CO_2 leakage during transport and storage. In contrast, the CO_2 mineralization process through carbonation presents a leakage-free and permanent sequestration method [2], which can be achieved either on-site through the use of combustion by-product and/or natural minerals, or off-site in a mineral mining place.

The on-site CO_2 mineralization usually occurs in a liquid medium, in which a mineral species is initially dissolved, and the resulting basic cations specifically calcium and/or magnesium are subsequently carbonated through bubbling the CO_2-containing flue gas into the leachate. Due to the relative easiness for scale-up [3], this route has been attracting plenty of attention worldwide [4]. The leaching media are either acidic reagents such as sulfuric acid (H_2SO_4), chloric acid (HCl), acetic acid, ammonium chloride (NH_4Cl) and ammonium sulfate ($(NH_4)_2SO_4$) or alkaline solutions such as sodium/potassium hydroxide (Na/KOH) [5,6]. Of these, acetic acid has been tested widely, principally due to the fact that it is prone to recycle and hence to increase the cost-effectiveness of the whole process [7], as demonstrated by the reactions:

$$\text{Extraction}: \quad CaO_{(s)} + 2CH_3COOH_{(aq)} \rightarrow Ca^{2+} + 2CH_3COO^- + H_2O_{(l)} \tag{1}$$

$$\text{Carbonation}: \quad Ca^{2+} + 2CH_3COO^- + CO_{2(g)} + H_2O \rightarrow CaCO_{3(s)} + 2CH_3OOH_{(l)} \tag{2}$$

To date, the parameters governing the leaching behavior of numerous minerals by reaction (1) have been examined extensively. The feedstock used includes natural mineral resources such as serpentine, wollastonite and olivine [8], and industrial wastes such as steelmaking slag [9], concrete [10] and fly ash derived from coal combustion and municipal solid waste incineration (MSWI) [11]. Of these, fly ash is potentially the most suitable source as it is generated on-site with CO_2 together in a combustion plant, thereby

* Corresponding author. Tel.: +61 3 9905 2592; fax: +61 3 9905 5686.
E-mail address: lian.zhang@monash.edu (L. Zhang).

0304-3894/$ – see front matter © 2012 Elsevier B.V. All rights reserved.
doi:10.1016/j.jhazmat.2012.01.053

Nomenclature

A	constant in Peng–Robinson equation [–]
A_s	exponential factor, s^{-1}
a	constant in Peng–Robinson equation [–]
B	constant in Peng–Robinson equation [–]
b	constant in Peng–Robinson equation [–]
E_a	activation energy, kJ/mol
f	fugacity, atm
k_s	rate constant of carbonation, s^{-1}
$n_{total\_CO_2,t}$	CO_2 reacted at time t during carbonation, mol/L
$n_{total\_CO_2,max}$	maximum CO_2 reacted at equilibrium during carbonation, mol/L
p	pressure, atm
R	ideal gas constant, kJ/mol K
T_c	critical temperature, K
T_r	relative temperature [–]
v	volume of gas, m^3
v_i	initial rate of CO_2 transfer, mol/s
z	compressibility factor [–]
Z	constant in Peng–Robinson equation [–]

Greek symbols

κ	constant in Peng–Robinson equation
ω	eccentric factor

requiring no transportation. In addition, its particle size is usually in the micro and sub-micron scale, thus requiring no comminution prior to being used. For the fly ash samples that have been tested in the literature, those bearing a relatively high concentration of calcium have proven effective in terms of carbon capture. However, as the mode of occurrence of calcium varies significantly with fly ash type and particle size, a generalized conclusion has yet to be achieved with respect to the optimum conditions for maximizing the elution of calcium upon leaching and its carbonation capacity. For instance, for calcium in a water–ash slurry system, its carbonation was optimized at a temperature of 30 °C and a pressure 4 MPa [12], which, however, is contradictory to the statement that carbonation efficiency is largely independent of the initial pressure of CO_2 as well as is little affected by reaction temperature [13].

Victorian brown coal is the single largest source meeting over 85% of the electricity needs in the State of Victoria, Australia. Due to its high moisture content, i.e. up to 75 wt%, the Victorian brown coal combustion exhibits a CO_2 emission rate of approximately 1300 kg-CO_2/MWh-electricity sent out, relative to ~900 kg-CO_2/MWh for the power plants burning high-rank black coal in Australia [14]. A carbon tax of AUD $23/tonne has been priced and to be implemented as of July 2012 in Australia. It is pivotal to develop a cost-effective PCC technique to be implemented shortly in the Latrobe Valley, Victoria, otherwise, the sustainability of brown coal and the whole industry in Victoria would be negatively impacted. The use of Victorian brown coal fly ash for CO_2 on-site mineralization has being tested by us, based on the consideration that, as a very young low-rank coal, Victorian brown coal is rich in alkali and alkaline earth metals [15]. The alkaline earth metals are highly concentrated in solid ash whereas the alkali metals preferentially vaporize into gaseous vapors leaving the chimney [15]. To date, approximately 1.3 million tons per annum fly ash is being produced in the Latrobe Valley, most of which is stored into ash dam as a waste. Changes to the local groundwater quality have been concerned [16]. The use of brown coal fly ash is expected to achieve a permanent capture of approximately 0.3 million tonnes CO_2 per annum, which concurrently leads to the production of calcium carbonate to be used as a value-added additive in local paper and pulp industry, thereby increasing the brown coal product diversification and creating new income stream. It is envisaged that, the CO_2 sequestration capacity of fly ash is not comparable to the total amount emitted in the Latrobe Valley. However, such a study is expected to act as 'icebreaker' for introducing CO_2 permanent mineralization technology that eventually may be picked up by the power producers. The mature technique for carbon capture using monoethanolamine (MEA) is highly sensitive to flue gas composition/quality and highly energy-demanding [17].

Table 1
Elemental composition of the Victoria brown coal fly ash tested here.

Element	Content (wt%)
CaO	29.7
MgO	25.5
SiO_2	9.2
Al_2O_3	2.5
Fe_2O_3	11.1
Na_2O	6.5
K_2O	0.5
SO_3	15.0
P_2O_5	0.03

In the present paper, the performance of a typical Victorian brown coal fly ash for CO_2 mineralization in acetic acid has been reported. As will be shown later, the brown coal fly ash derived leachate is dominated by the co-existence of calcium and magnesium, rather than mainly one metal in a natural mineral-derived leachate. Parametric investigation and intensive characterization have been conducted to clarify the influences of individual factors on the carbonation efficiency of these two metals and the properties of the resulting carbonates. In addition, kinetic modeling has been carried out to extract the activation energy and compare it with other carbon capture sources.

2. Experimental work

2.1. Victorian brown coal fly ash properties

The fly ash tested here is a dry ash sample collected directly from an electrostatic precipitator in International Power Hazelwood Pty Ltd., which provides approximately 33% of the electricity needs in Victoria. As indicated in Table 1, the sample tested includes 30 wt% CaO and 25.8 wt% MgO. The total amount of these two oxides is far higher than in a bituminous coal fly ash which is overwhelmingly dominated by Al/Si oxides. Moreover, as determined by computer-controlled scanning electron microscopy (CCSEM) by the methodologies explained elsewhere [18], the ash sample tested here is very fine in particle size, most of which fall into the size bins of 2.2–4.6 μm and 4.6–10 μm, see Fig. 1. Both calcium and magnesium are also mainly present in these two size bins. These size bins are even smaller than the optimum size range of 20–150 μm for maximum carbon capture mentioned in the literature [12]. It is desirable that the dissolution rate of this fly ash sample is very fast as well as highly cost-effective as the comminution for coarse particle is unnecessary.

2.2. Fly ash leaching in acetic acid and carbonation conditions

According to the reaction Eqs. (1) and (2) shown above, the acetic acid was used to dissolve fly ash. The resulting leachate was subsequently bubbled by CO_2 for carbonation. Simultaneously, the acetic acid was regenerated. The conditions including 6% (v/v) acetic acid, a liquid to solid ratio of 10 and stirring duration of 1 h were used for ash leaching at ambient conditions, resulting in the extraction of the majority of calcium and magnesium into the leachate, in which the other elements are much lower and even under the detection limit

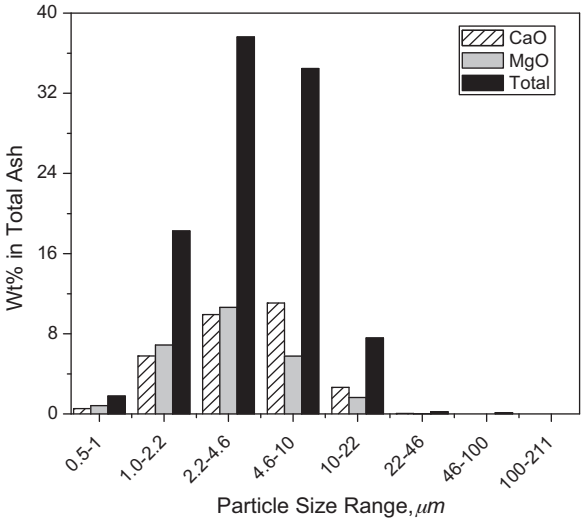

Fig. 1. Particle size distribution of overall fly ash and CaO and MgO determined by CCSEM.

of the inductively coupled plasma optical emission spectroscopy (ICP-OES, PerkinElmer 7100DV), as shown in Table 2.

Carbonation of fly ash leachate was conducted in a batch-scale continuously stirred high-pressure autoclave (BR-300, Berghof) with a capacity of 300 mL. For each run, approximately 50 mL leachate was firstly poured into a Teflon beaker, which was then placed into the autoclave under immediately mechanical stirring and heated up to the desired temperature at a heating rate of approximately 5 °C/min. Note that, the autoclave was protected by inert nitrogen in the heating stage. Once the temperature was reached, the pure CO_2 (Grade 4.5 Linder gas) was injected at a certain pressure, and the reaction was then held for a certain period. Eventually, the system pressure was released, and the solution was filtrated using ADVENTEC filter GC-50 under vacuum. The resulting solid powders were dried at 105 °C overnight and stored for analysis.

Considering that the soluble bicarbonate can also be formed during carbonation, the pressure drop of CO_2 over time was monitored real-time to estimate its consumption rate. A control experiment for blank solution containing no cations was also conducted. The CO_2 consumed by the carbonation of the fly ash-derived leachate was calculated according to [13]

$$P_{\text{carbonation}} = P_{\text{global}} - P_{\text{blank solution}} \tag{3}$$

Fig. 2 shows a typical pressure drop caused by the carbonation of fly ash leachate and black solution at 80 °C and 10 bar. The resulting $P_{\text{carbonation}}$ was converted to the quantity of CO_2 consumed [13]:

$$n_{CO_2} = \frac{P_{\text{carbonation}} V}{RT} \tag{4}$$

Table 2
Concentrations of the elements dissolved in the leachate.

Element	Content (g/L)
Ca^{2+}	14
Mg^{2+}	7
Fe^{3+}	0.3
Al^{3+}	1
Mn	0.2
Si	<0.2
Cr	<0.0002
Cd	ND
As	ND
SO_4^{2-}	0.02

ND: non-detectable

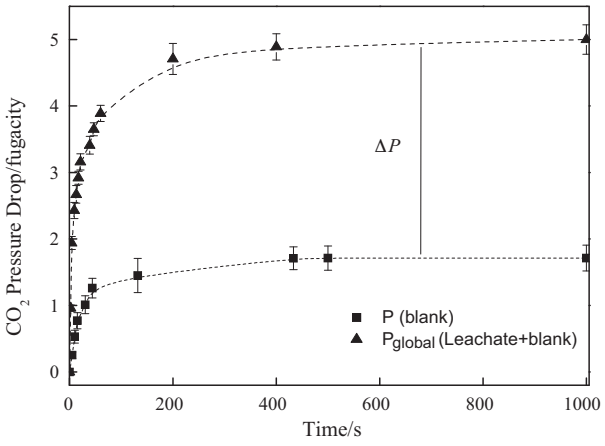

Fig. 2. CO_2 pressure drop between leachate and black solution.

where V is the volume that occupied by gas, T is temperature of reaction, and R gas constant (0.008314 kJ mol^{-1} K^{-1}). Here, the pressure P needs to be replaced by fugacity, considering the deviation of the properties of CO_2 from an ideal gas at the high pressure adopted here. The Peng–Robinson equation was used to determine fugacity and compressibility factor for CO_2 according to:

$$p = \frac{RT}{v-b} - \frac{a(T)}{v(v+b)+b(v-b)} \tag{5a}$$

$$Z^3 - (1-B)Z^2 + (A - 3B^2 - 2B)Z - (AB - B^2 - B^3) = 0 \tag{5b}$$

$$a(T) = a(T_c) \times \alpha(T_r, \omega) \tag{5c}$$

$$a^{1/2} = 1 + \kappa(1 - {T_r}^{1/2}) \tag{5d}$$

$$\kappa = 0.37464 + 1.54226\omega - 0.26992\omega^2 \tag{5e}$$

$$\alpha(T_r, \omega) = [1 + \kappa(1 - {T_r}^{1/2})]^2 \tag{5f}$$

$$\ln\frac{f}{p} = Z - 1 - \ln(Z-B) - \frac{A}{2\sqrt{2}B}\ln\frac{Z + 2.414B}{Z - 0.414B} \tag{5g}$$

where

$$A = \frac{aP}{R^2T^2}; \quad B = \frac{aP}{RT}; \quad Z = \frac{Pv}{RT}. \tag{5h}$$

A convergence function was then formed:

$$f(Z) = \exp(Z - 1 - \ln(Z-B)) - \frac{A}{(2 \times B \times \sqrt{2})} \times \ln\frac{(Z + (1+\sqrt{2}) * B)}{(Z + (1-\sqrt{2}) * B)} \tag{6}$$

The parameters of CO_2 in Peng–Robinson equation as shown in the literature [19] were adopted.

Extra experiments were also carried out for the direct carbonation of fly ash as a form of ash–water slurry to compare with the indirect method proposed here. The ash–water slurry has being tested by the existing power plant for a temporary storage of CO_2 after it is purified by MEA from flue gas. A typical condition of temperature 60 °C, initial CO_2 pressure 10 bar, stirring speed 400 rmp and stirring time 60 min has been tested and compared with the ash-derived leachate.

2.3. Characterization of leachate and solid species

For both fresh and used leachate, the concentrations of cations were quantified using ICP-OES. In the meanwhile, a variety of techniques were used to characterize the carbonation precipitates, including X-ray Fluorescence Spectrometry (XRF, Rigaku-2100) for elemental composition, X-ray diffraction (XRD, Rigaku RINT) for

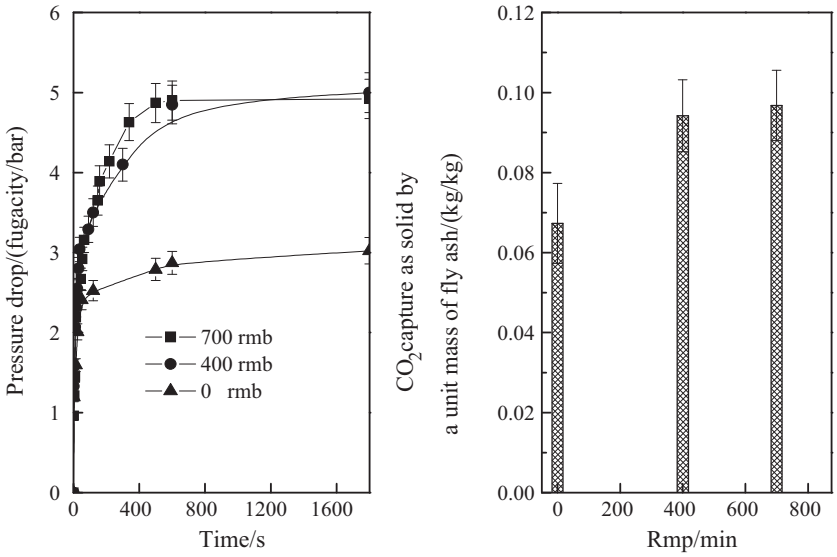

Fig. 3. Effect of stirring speed on carbonation pressure drop and precipitate yield at 20 °C for 30 min and 10 bar.

crystallized structure identification using a diffractometer with a Cu-Kα radiation at a wavelength of λ = 1.5406 Å, and scanning electron microscopy (SEM, JEOL5600) for morphology observation and particle size measurement. For SEM observation, the sample powder was first dispersed into ethanol by ultra-sonication in 5 min. The resulting slurry was then dropped onto a piece of carbon tape, dried at 50 °C, and finally carbon-coated prior to microscopic observation. For particle size counting, more than 100 particles were observed and their diameters were measured by Image-Pro 6.2. Thermal gravimetric analysis was also conducted by TG-DTA851 to quantify the loss-on-ignition (LOI) of the carbonation precipitate by heating a sample up to 900 °C in nitrogen.

3. Results and discussion

3.1. Influences of autoclave stirring speed

Effect of stirring speed of the autoclave on CO_2 capture was firstly studied under the conditions of room temperature, 10 bar CO_2 and 30 min. As demonstrated in the left panel of Fig. 3, the pressure drop was equilibrated at approximately 2–3 bar for the case without stirring, which was quickly stabilized at ~5 bar in 10 min with stirring. The comparison here is a clear sign of a poor mass transfer for CO_2 into leachate. The right panel of Fig. 3 for the amount of CO_2 captured as solid precipitate also substantiates that, a continuous stirring at 400 rmp is sufficient for minimizing/eliminating the diffusion limit for CO_2 capture in the batch-scale autoclave reactor adopted here.

3.2. Influence of carbonation temperature

The influence of carbonation temperature was investigated secondly under a typical condition of 10 bar CO_2 and 30 min stirring at 400 rmp. Fig. 4 illustrates the quantity of CO_2 captured by a unit mass of fly ash on two aspects: CO_2 pressure drop calculated by Eqs. (3)–(6), and solid precipitate amount collected after filtration. Interestingly, the calculation gave a much higher estimate than the corresponding solid mass. Clearly, apart from solid precipitate, water-soluble species were also form to bind CO_2, which is principally Mg bicarbonate, as will be further explained later. In addition, Fig. 4 demonstrates that, for either CO_2 is captured in solid or liquid phase, the CO_2 capture capacity of the fly ash sample is maximized at 60 °C. A further increase in temperature from 60 °C onwards resulted in insignificant change or slight if not negligible drop on the mass of CO_2 captured. This can be partly explained by the fact that mineral carbonation is an exothermic process which is negatively affected at elevated temperatures. Moreover, increasing temperature plays a detrimental role on the solubility of CO_2 in an aqueous solution, which in turn inhabits the carbonation extent.

The XRD spectra for the precipitates are illustrated in Fig. 5, where pure calcite ($CaCO_3$) and dolomite ($CaMg(CO_3)_2$), were also included for comparison. The angles of 25–35° were amplified as inset in Fig. 5. For the room temperature precipitate, its strongest peak centering at ~30° overlaps largely with that of pure calcite. A remarkable right shift was however noticed upon the increase in the temperature. For the spectrum of the precipitate formed at 80 °C, the strongest peak was formed at 30.88°, which is much closer to dolomite ($CaMgCO_3$) than calcite. The broad width of this peak and others centering at higher degrees also imply the slight discrepancy between the 80 °C precipitate and pure dolomite, which can be caused by the presence of trace calcite and/or the distinct diffraction orientation of the carbonation precipitated formed here. The TGA and XRF results in Table 3 indicate the LOI values of 41–42 wt% for the precipitates formed, which are close to the quantity of 44% CO_2 in calcite. With the increase in reaction temperature, the CaO content in precipitate dropped evidently, in comparison to a continuous increase for the content of MgO. A molar ratio of

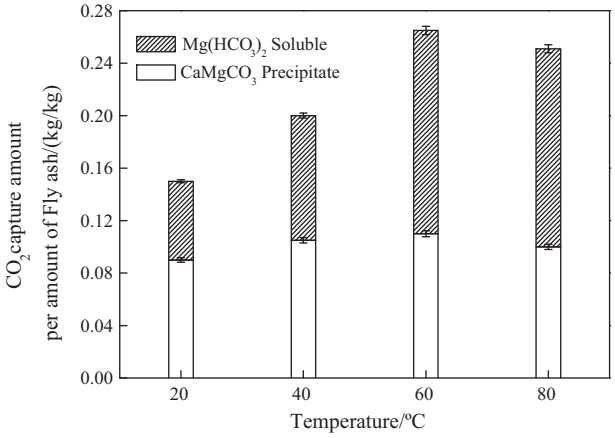

Fig. 4. Effect of carbonation temperature on CO_2 capture capacity at 10 bar.

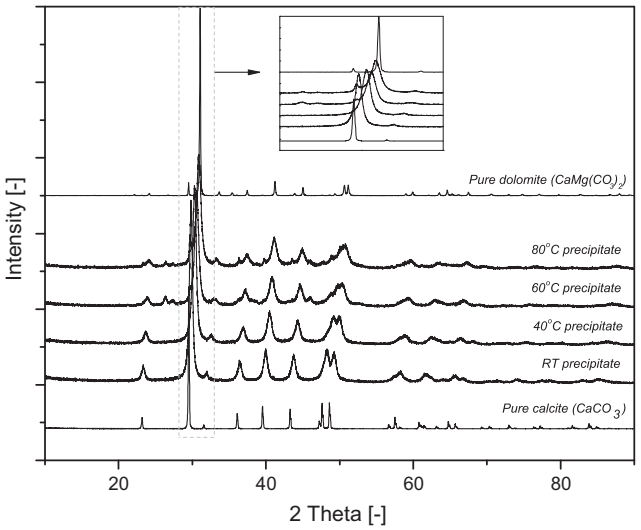

Fig. 5. XRD of precipitate at different temperatures for 60 min at 10 bar.

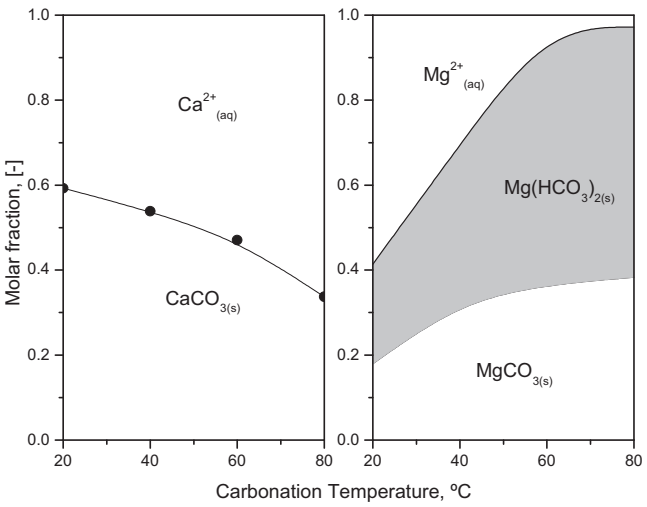

Fig. 6. Conversion of different carbonates during carbonation at different temperatures.

1.05 for CaO to MgO has been achieved at 80 °C, which is obviously dolomite. The incorporation of Mg into dolomite at 80 °C should be caused by the decomposition of its water-soluble bicarbonate.

The bubbling of gaseous CO_2 into fly ash leachate is initiated by its dissolution to form HCO^{3-} by Eq. (7), which subsequently dissolves to form CO_3^{2-} by Eq. (8). For the optimized stirring speed 400 rmp adopted here, these two reactions are apparently fast and exert very limited influence on the overall carbonation rate. For the CO_3^{2-} anion formed, its stabilization follows reaction (9) for the formation of calcium carbonate. Such a reaction is exothermic and hence, it is depreciated at elevated temperatures. In contrast, for magnesium ion, it initially reacts with HCO^{3-} rather than CO_3^{2-} to form Mg bicarbonate which is highly water-soluble, according to Eq. (10). Upon heating, the resulting bicarbonate is expected to decompose into carbonate and release one molar CO_2 as gas by Eq. (11). This explains a gradual increment on the content of Mg in the solid precipitate in Table 3.

$$CO_2(aq) + OH^- \rightarrow HCO_3^- \quad (7)$$

$$HCO_3^- + OH^- \rightarrow CO_3^{2-} + H_2O \quad (8)$$

$$Ca^{2+} + CO_3^{2-} \rightarrow CaCO_3\downarrow \quad (9)$$

$$Mg^{2+} + 2HCO_3^- \rightarrow Mg(HCO_3)_2 \quad (10)$$

$$Mg(HCO_3)_2 \xrightarrow{\nabla} MgCO_3\downarrow + H_2O + CO_2 \quad (11)$$

Following the discussions on Figs. 4 and 5 and Table 3, the fate of both Ca and Mg ions upon carbonation in acetic acid solution are elucidated quantitatively. Fig. 6 plotted the fraction of each ion converted to carbonate/bicarbonate versus carbonation temperature. Here again, the decrease in the fraction of Ca carbonate with increasing temperature is evident, substantiating the exothermic nature of reaction Eq. (9). The un-reacted Ca^{2+} ratio is remarkably higher, varying from 0.4 at 20 °C to 0.6 at 80 °C. This is an indicator of the favored backward reaction of Eq. (2) for the dissolution of $CaCO_3$ into acetic acid. Regarding Mg, its carbonation ratio was improved stably with the increase in temperature, reaching from approximately 0.4 at 20 °C to 0.97 at 80 °C. The formation of water-soluble Mg bicarbonate was promoted more pronouncedly than the carbonate precipitate. This supports a slow reaction rate of Eq. (11) for the decomposition of Mg bicarbonate.

Table 3
Elemental compositions of the precipitates formed under the carbonation condition of 10 bar CO_2 and 30 min, wt%.

	RT	40 °C	60 °C	80 °C
LOI	41.9	42.0	42.1	42.1
CaO	44.8	39.3	36.5	30.9
MgO	8.1	14.1	16.9	20.9
SiO_2	1.7	1.5	1.5	2.3
Al_2O_3	0.6	0.5	0.6	0.8
Fe_2O_3	1.6	1.7	1.3	1.6
Na_2O	0.7	0.5	0.7	0.7
K_2O	0.04	0.05	–	0.05
SO_3	0.5	0.3	0.3	0.6

The co-precipitation of two carbonates favors particle agglomeration and their filtration. As demonstrated in Fig. 7(a), for the precipitate formed at room temperature, it exhibits a most probable size of approximately 0.95 μm. A bimodal distribution with two peaks of 2.0 and 5.0 μm were formed at 40 °C. A further increase on the temperature to 60 °C shifted the whole distribution to larger size range with two peaks centering at 8.5 and 12.0 μm respectively. Since no further shift was observed at 80 °C, it is conclusive that 60 °C is the optimum temperature for carbonate agglomeration, which is also the best temperature for maximizing the quantity of CO_2 captured, as demonstrated in Fig. 4. The particle morphologies in panels (b) and (c) also demonstrates the predominance of rod-like crystals with fine size and sharp edge in the 25 °C precipitate, which is calcite as indicated in Fig. 5. Instead, the single particles formed at 80 °C are mainly in round shape and agglomerated noticeably. The change in the crystal shape is an extra evidence of the incorporation of Mg into calcite which losses the crystal edges accordingly. This may also explain the slight discrepancy between 80 °C precipitate and natural dolomite in terms of the XRD peak position and width in Fig. 5.

3.3. *Influence of CO_2 partial pressure*

For a given reaction period of 60 min at 60 °C, the results in Fig. 8 indicate the insignificant variation of the quantity of CO_2 captured as solid with CO_2 partial pressure. This further substantiates the above hypothesis that CO_2 diffusion is not a limit control step for carbonation in the continuously stirred autoclave used here, provided that the reaction time is longer enough for the equilibrium of Eqs. (9)–(11) to be achieved.

The XRD spectra in Fig. 9 demonstrate the preferential formation of high-purity calcium carbonate at the elevated CO_2 pressure. With the CO_2 pressure increasing, the major peak centering on approximately 29.8° continued to shift left towards an angle which

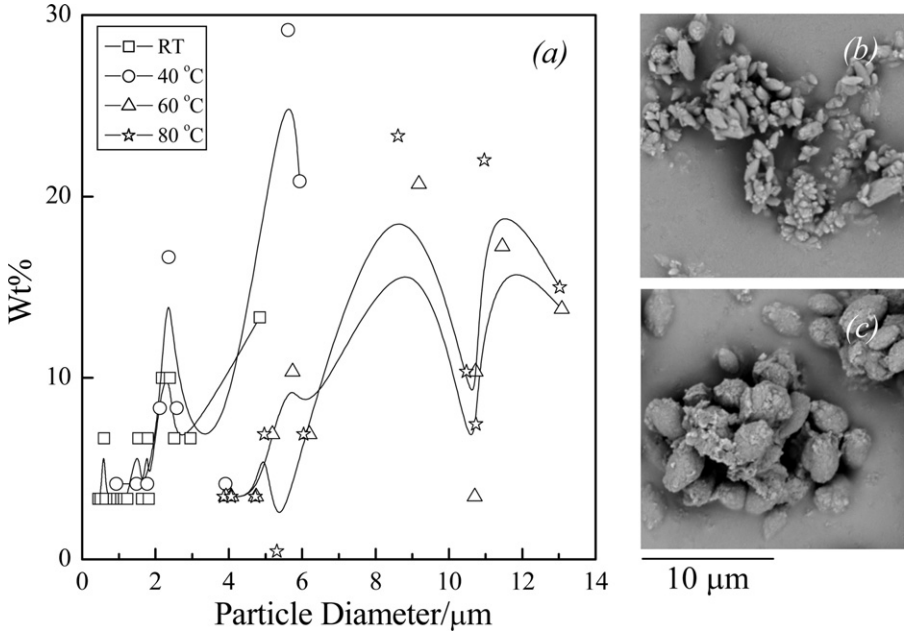

Fig. 7. Particle size distribution (a) and morphologies ((b) for room temperature and (c) for 80 °C) of precipitates formed at different temperatures.

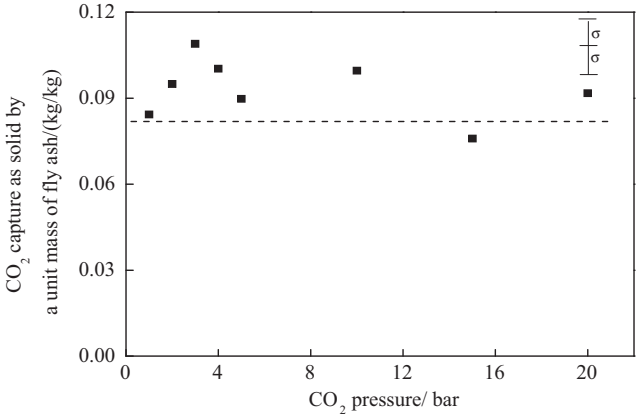

Fig. 8. Effect of CO_2 pressure on CO_2 capture as solid precipitate at 60 °C.

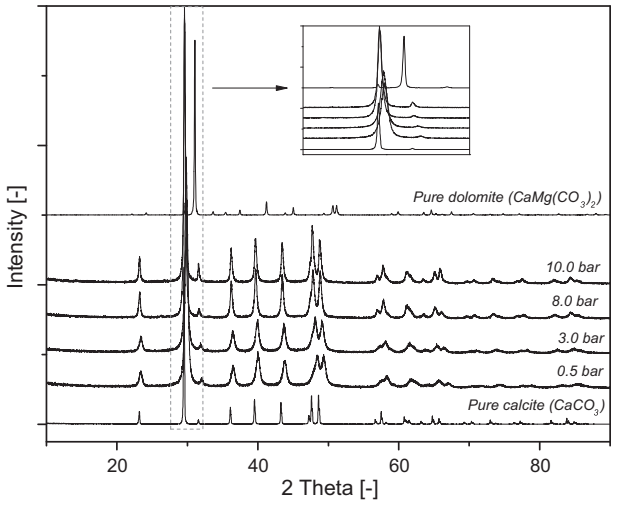

Fig. 9. XRD spectra for the precipitates formed versus CO_2 partial pressure.

is representative of pure calcite. The content of Mg in the precipitate was reduced noticeably. This is the evidence for the promotion of reaction Eq. (9) whereas the inhibition of the forward reaction for Eq. (11) upon the increase in the CO_2 partial pressure.

The initial CO_2 pressure is also influential in terms of carbonate formation rate. As expected, for a CO_2 pressure less than 1 bar, the carbonation reactions (9)–(11) would be lengthy. The increase in the initial CO_2 pressure clearly favors its dissolution and diffusion into the fly ash-derived leachate. Here, a pseudo-second-order kinetic model was used to simulate the CO_2 carbonation rate [13].

$$\frac{dn_{\text{total\_CO}_2,t}}{dt} = k_s(n_{\text{total\_CO}_2,\max} - n_{\text{total\_CO}_2,t})^2 \quad (12)$$

where k_s is the rate constant of sequestered CO_2 for a given initial CO_2 pressure and a given temperature, the $n_{\text{total\_CO}_2,\max}$ is the maximum quantity of CO_2 sequestered at equilibrium (mol), $n_{\text{total\_CO}_2,t}$ is the sequestrated quantity of CO_2 at t seconds. The initial rate of CO_2 transfer v_i (mol/s) in the system can be calculated by [13]:

$$v_i = k_s(n_{\text{total\_CO}_2,\max})^2 \quad (13)$$

Fig. 10 depicts the initial rate of CO_2 transfer as a function of the initial CO_2 pressure. As demonstrated, increasing pressure is beneficial for increasing the initial rate of transfer for CO_2. However, since a pressurized vessel is difficult to operate and is also costly, the result in Fig. 8 is a clear indicator that increasing reaction time is beneficial for compensating the promoting effect of CO_2 partial pressure.

3.4. Kinetic modeling of CO_2 transfer in leachate during carbonation

The pseudo-second-order kinetic model was further used to model the CO_2 capture rate in the given reaction system, which is described in Eq. (14). This differential equation was integrated with analytical approach together for an initial condition of $n_{\text{total\_CO}_2,t} = 0$ at $t = 0$:

$$n_{\text{total\_CO}_2,t} = \frac{n_{\text{total\_CO}_2,\max} \times t}{(k_s \times n_{\text{total\_CO}_2,\max})^{-1} + t} \quad (14)$$

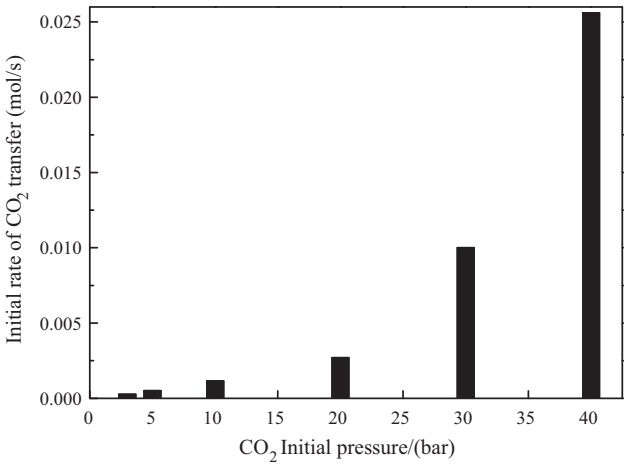

Fig. 10. Effect of CO_2 partial pressure on the initial rate of CO_2 transfer.

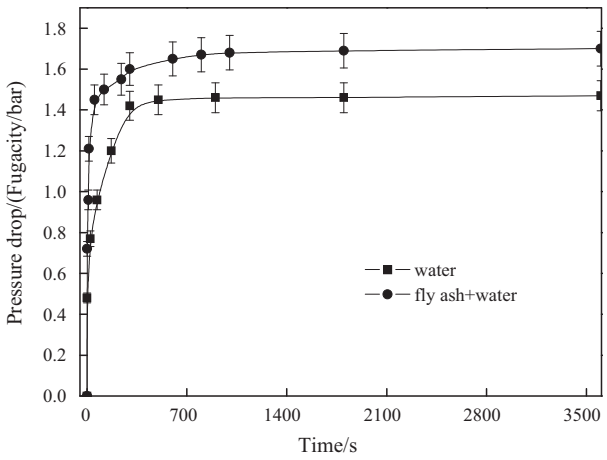

Fig. 13. Pressure drop during the carbonation of fly ash–water slurry.

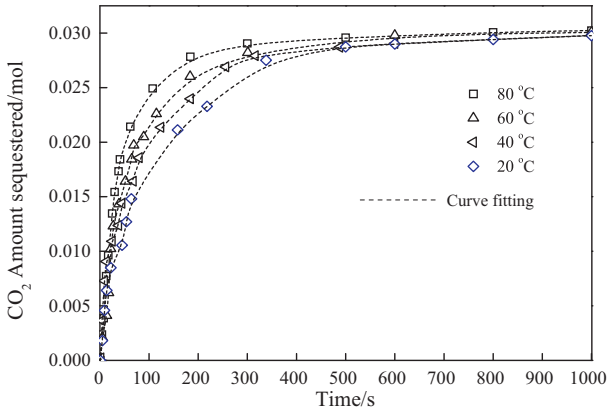

Fig. 11. Sequestration kinetics at different temperatures with a CO_2 partial pressure at 10 bar.

The fminsearch function in MATLAB was used for the fitting of experimental results via the error minimization algorithm. An excellent agreement between fitting and experimental observation for a relative variance R^2 over 0.98 has been confirmed, see Fig. 11.

The obtained rate constant at different temperatures can be expressed through Arrhenius law (Fig. 12):

$$k_s = A_s \times e^{-E_a/RT} \quad (15)$$

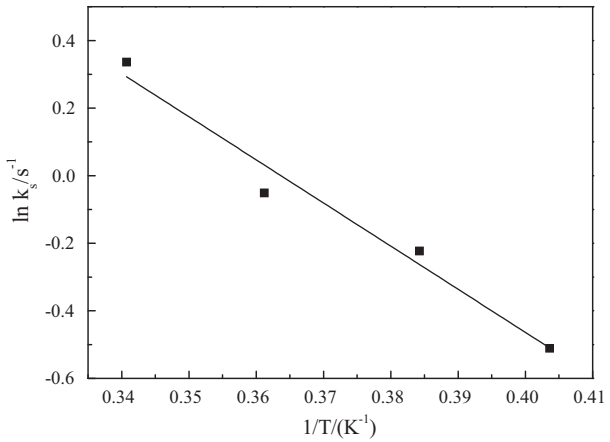

Fig. 12. Activation energy for carbonation with an initial CO_2 partial pressure of 10 bar.

where A_s is the pre-exponential factor (s^{-1}), R is gas constant (0.008314 kJ mol^{-1} K^{-1}), T is experimental temperature (K), and E_a the activation energy of carbonation (kJ/mol). The calculated apparent activation energy was found to be 12.7 kJ/mol with a relative variance R^2 over 0.96 for the carbonation of calcium and magnesium ions in the brown coal fly ash leachate. Such a figure falls between the value for the apparent activation energy obtained from aqueous $Ca(OH)_2$ carbonation, 9.92 kJ/mol [20] and that for carbonation of aqueous $Mg(OH)_2$ solution, 54 kJ/mol [21]. This further confirms the involvement of Eqs. (9)–(11) for the carbonation of the brown coal fly ash-derived leachate tested here. In addition, according to the literature report [22], the apparent activation energy of gas–solid reaction between CaO and CO_2 over 400 °C is 180 kJ/mol and 98 kJ/mol for the absence and presence of 15% water in the reaction system, respectively, which is much higher than our results achieved in aqueous solution. It is also noteworthy that, the apparent activation energy achieved here is comparable to potassium carbonate with piperazine which has a heat of adsorption of 42–63 kJ/mol CO_2 [23]. Since the overall chemistry for carbonation is exothermic and brown coal fly ash is small enough for no comminution requirement, the system developed here could operate at zero or negative energy input. It is thus a very energy-saving and efficient process when compared with the high-temperature gas–solid carbonation process.

3.5. Comparison between this study and the ash–water carbonation system

After being collected from electrostatic precipitator, the Victorian brown coal fly ash is mixed with water and pumped as slurry into ash storage dam. The ash–water slurry is being used directly for the storage of CO_2 after flue gas separation in the Latrobe Valley. Extra effort was thus made to compare our process with this existing system. As demonstrated in Fig. 13, a pressure drop of 0.25 bar CO_2 has been achieved for the ash–water slurry system, which is much lower than that achieved for the fly ash acetic acid leachate, ~3 bar shown in Fig. 2. This is mainly attributed to the immobilization of Ca and Mg in the original fly ash matrix, which is less reactive unless being liberated. Based upon the net CO_2 consumed, it is referable that, the quantity of CO_2 captured by ash–water slurry reached 26.4 kg/tonne fly ash, which is 37.9 tonne mineral/tonne CO_2 in terms of the concept R_{CO_2}, a theoretical mineral mass necessary to bind a unit mass of CO_2 as carbonate. In contrast, for the system developed by us, by taking both contributions of solid carbonates and water-soluble bicarbonate into account, the maximum CO_2 capture capacity reached 264 kg/tonne fly ash and 3.79 tonne

Table 4
Comparison of the CO_2 capture capacity of natural minerals and various fly ashes.

Carbonation condition	CO_2 capture capacity, (kg CO_2/tonne fly ash)	Fly ash type	Reference
36 °C, 10 bar suspensions 579 h	46	Lignite fly ash	[11]
36 °C, 10 bar suspensions with shaking 614 h	78	Lignite fly ash	[11]
30 °C 40 bar, 2 h together with brine	71.8	Black coal fly ash	[12]
25 °C, 40 bar, 2 h	26.2	Black coal fly ash	[13]
43 °C, 1 bar, 2 min, in fluidized bed	11	Black coal fly ash	[25]
25 °C, 10 bar, 1 h	26.4	Victorian brown coal fly ash–water slurry	This work
This study at 60 °C 10 bar, 1 h	123	Victorian brown coal fly ash	This work
This study at 60 °C 10 bar, 1 h	264[a]	Victorian brown coal fly ash	This work

[a] Refers to the calculation with $Mg(HCO_3)_2$ inclusive.

mineral/tonne CO_2 equivalent, which is ten-folds larger than the ash–water slurry system. It is also comparable to the capture capacity of a variety of natural minerals with the R_{CO_2} typically ranging from 1.8 to 3.0 tonne mineral/tonne CO_2 [24]. Even in the case that the magnesium bicarbonate is excluded, a maximum CO_2 capture capacity of 123 kg CO_2/tonne fly ash is also achievable, which is still significantly higher than the other fly ash samples summarized in Table 4. For the fly ash rich in aluminum and silicon, a maximum capture capacity of 26.2 kg CO_2/tonne fly ash and 11 kg CO_2/tonne fly ash are achievable, which is just comparable to the brown coal fly ash-waster slurry system.

4. Conclusions

Intensive investigation on the propensity of a brown coal fly ash-driven acid-soluble alkaline earth metals on CO_2 fixation by carbonation has been conducted in this paper. Apart from parametric investigation on the influence of stirring speed, carbonation temperature and CO_2 partial pressure, kinetic simulation has also been carried out to explore the fundamental knowledge governing the co-carbonation of calcium and magnesium cations in acetic acid solution. The major conclusions are drawn as follows:

(1) The co-existence of calcium and magnesium irons in aqueous solution captured the CO_2 in both solid carbonate precipitate and water-soluble magnesium bicarbonate. Increasing temperature deteriorated the carbonation of calcium, whereas it favored the decomposition of magnesium bicarbonate into carbonate precipitate. In contrast, increasing CO_2 partial pressure is beneficial for increasing the purity of calcium carbonate by inhibiting the precipitation of magnesium as carbonate.
(2) The magnesium carbonate preferentially co-precipitated with calcium carbonate together into micron-scale aggregates, the size of which varies noticeably with carbonation temperature.
(3) A global activation energy of 12.7 kJ/mol during carbonation has been confirmed for the brown coal fly ash acid-soluble alkaline earth metals, which is highly energy-efficient. The maximum capacity of the system developed here can reach 264 kg CO_2/tonne fly ash. Such a capacity is substantially higher than the direct carbonation of ash–water slurry and comparable to a variety of natural mineral resources.

Acknowledgments

The authors are grateful to the Faculty of Engineering of Monash University for the financial support through a 2011 new staff member research grant. Mr Facun Jiao and Professor Yoshihiko Ninomiya at Chubu University of Japan are acknowledged for the XRF and XRD analysis. The use of TGA at Prof Paul Webley's laboratory in the Department of Chemical Engineering, Monash University is also highly appreciated.

References

[1] K.S. Lackner, A guide to CO_2 sequestration, Science 300 (2009) 1677–1678.
[2] H. Herzog, Carbon Sequestration via Mineral Carbonation: Overview and Assessment, MIT Laboratory for Energy and the Environment, USA, 2002, pp. 1–10.
[3] J. Sipila, S. Teir, R. Zevenhoven, Carbon dioxide sequestration by mineral carbonation literature review update 2005–2007, Reports, Faculty of Technology, Finland, 2008.
[4] W.J. Bao, H.Q. Li, Y. Zhang, Selective leaching of steelmaking slag for indirect CO_2 mineral sequestration, Industrial and Engineering Chemistry Research 49 (2010) 2055–2063.
[5] S. Teir, H. Revitzer, S. Eloneva, C.J. Fogelholm, R. Zevenhoven, Dissolution of natural serpentinite in mineral and organic acids, International Journal of Mineral Processing 83 (2007) 36–46.
[6] S. Teir, R. Kuusik, C.J. Fogelholm, R. Zevenhoven, Production of magnesium carbonates from serpentinite for long-term storage of CO_2, International Journal of Mineral Processing 85 (2007) 1–15.
[7] M. Kakizawa, A. Yamasaki, Y. Yanagisawa, A new CO_2 disposal process via artificial weathering of calcium silicate accelerated by acetic acid, Energy 26 (2001) 341–354.
[8] S.J. Gerdemann, W.K. O'Connor, D.C. Dahlin, L.R. Penner, H. Rush, Ex situ aqueous mineral carbonation, Environmental Science & Technology 41 (2007) 2587–2593.
[9] W.J.J. Huijgen, G.J. Witkamp, R.N.J. Coman, Mineral CO_2 sequestration by steel slag carbonation, Environmental Science & Technology 39 (2005) 9676–9682.
[10] I. Galan, C. Andrade, P. Mora, M.A. Sanjuan, Sequestration of CO_2 by concrete carbonation, Environmental Science & Technology 44 (2010) 3181–3186.
[11] A. Uliasz-Bochenczyk, E. Mokrzycki, Z. Piotrowskib, R. Pomykala, Estimation of CO_2 sequestration potential via mineral carbonation in fly ash from lignite combustion in Poland, Energy Procedia 1 (2009) 4873–4879.
[12] M. Nyambura, G. Mugera, P. Felicia, N. Gathura, Carbonation of brine impacted fractionated coal fly ash: implications for CO_2 sequestration, Journal of Environmental Management (92) (2011) 655–664.
[13] G. Montes-Hernandez, R. Perez-Lopez, F. Renard, J.M. Nieto, L. Charlet, Mineral sequestration of CO_2 by aqueous carbonation of coal combustion fly-ash, Journal of Hazardous Materials 168 (2009) 31–37.
[14] http://www.envict.org.au/file/Greenhouse_Brown_Coal_05.pdf.
[15] C.Z. Li (Ed.), Advances in the Science of Victorian Brown Coal, Elsevier, 2004, pp. 37–45.
[16] G.M. Mudd1, T.R. Weaver, J. Kodikara, T. McKinley, Groundwater chemistry of the Latrobe Valley influenced by coal ash disposal. 1: Dissimilatory sulphate reduction and acid buffering, in: International Association of Hydrogeologists Conference: Groundwater: Sustainable Solutions, Melbourne, VIC, February, 1998.
[17] P. Feron, B. Hooper, M. Attala, N. Dave, S. Kentish, G. Stevens, L. Wardhaugh, P. Webley, Research opportunities in post combustion CO_2 capture, in: Scoping study for Australian National Low Emission Coal R&D program (ANLEC R&D), Australia, October, 2009, http://www.anlecrd.com.au/publications.
[18] D. Yu, M. Xu, L. Zhang, H. Yao, Q. Wang, Y. Ninomiya, Computer-controlled scanning electron microscopy (CCSEM) investigation on the heterogeneous nature of mineral matter in six typical Chinese coals, Energy & Fuels 21 (2) (2007) 468–476.
[19] Y. Sun, G. Yang, J.P. Zhang, Y.S. Wang, M.S. Yao, Preparation of activated carbon from spend acid precipitated corn stover lignin by phosphoric acid activation and its application for gas separation, Chemical Engineering and Technology 35 (2) (2012) 309–316.
[20] V.V. Zedtwitz-Nikulshyna, CO_2 capture from atomspheric air via solar driven carbonation calcination cycle, PhD Thesis, 2009, pp. 48–49.

[21] Q.F. Hu, Production and Application of Magnesium Related Compounds, second ed., Chemical Industrial Press, Beijing, 2004, pp. 218–220.
[22] V. Nikulshina, M.E. Galvez, A. Steinfeld, Kinetic analysis of the carbonation reactions for the capture of CO_2 from air via the $Ca(OH)_2$–$CaCO_3$–CaO solar thermochemical cycle, Chemical Engineering Journal 129 (2007) 75–83.
[23] http://www.netl.doe.gov/publications/factsheets/project/Proj280.pdf.
[24] R. Zevenhoven, J. Fagerlund, J.K. Songok, CO_2 mineral sequestration: developments towards large-scale application, Greenhouse Gas Science and Technology 1 (2011) 48–57.
[25] K.J. Reddy, S. John, H. Weber, M.D. Argyle, P. Bhattacharyya, D.T. Taylor, M. Christensen, T. Foulke, P. Fahlsing, Simultaneous capture and mineralization of coal combustion flue gas carbon dioxide (CO_2), Energy Procedia 4 (2011) 1574–1583.